Ecological Informatics 92 (2025) 103517

Contents lists available at ScienceDirect

Ecological Informatics

journal homepage: www.elsevier.com/locate/ecolinf

Automatic fish scale analysis: age determination, annuli and circuli detection, length and weight back-calculation of coregonid scales

Christian Vogelmann [a,b,*], Christian Schock [c], Marius Feilhauer [d], Herwig Stibor [a], Michael Schubert [b]

[a] *Ludwig-Maximilians-Universität München, Faculty of Biology Department II, Aquatic Ecology, Großhaderner Str. 2, 82152 Planegg-Martinsried, Germany*
[b] *Bavarian State Research Center for Agriculture (LfL), Institute for Fisheries, Weilheimer Str. 8, 82319 Starnberg, Germany*
[c] *Independent Engineer, Schorndorf, Germany*
[d] *Independent Engineer, Urbach, Germany*

ARTICLE INFO

Keywords:
Age determination
Automated scale analysis
Digitization
Length and weight back-calculation

ABSTRACT

Age determination and growth measurment through scale analysis offer valuable insights into fish population structure and growth history, providing indications of abiotic, anthropogenic, or evolutionary influences. Traditional scale analysis is time-consuming and reliant on expert personnel. This study introduces an automated or semi-automated approach for analyzing coregonid scales, highlighting the benefits of digitization. Compared to manual stereomicroscope examination, software-assisted analysis enables reproducible and independent evaluation. Biometric features such as scale area, radius, circuli count, and spacing can be measured faster. Automatic detection of the scale center and standardized determination of the longest radius allow for efficient back-calculation of fish length, weight, and age. Two independent datasets were used to assess the performance of the automated system. Results from paired validation analyses (n = 84 scales) demonstrate high agreement between automated and manual measurements for scale area ($r = 0.97$, $r^2 = 0.95$) and circuli count ($r = 0.78$, $r^2 = 0.60$). In a larger field application dataset (n = 1095 scales from 124 fish), the automated algorithm identified the scale center without manual correction in 77.9 % of cases. For the remaining 22.1 %, the mean correction was only 0.15 mm (median: 0 mm), and just 7.6 % required a correction greater than 0.5 mm. Deviations between fully automated and manually verified results for circuli count, radius length, circuli spacing, and age determination were consistently low, supporting robust performance under real-world monitoring conditions. All quantitative metrics are reported in detail in the study. Back-calculated length and weight across age classes were consistent between methods.

Manual processing of 84 scales required approximately 16 working hours, whereas the automated workflow—including scanning and analysis—was completed in under three hours. For the complete field dataset of 1095 scales, automated analysis required only a few minutes after scanning, while full manual verification was completed in less than two hours. These results demonstrate a substantial gain in efficiency, enabling highly standardized, reproducible, and large-scale application of scale analysis in ecological monitoring and fisheries management.

1. Introduction

Scale analysis has long been a valuable tool in fisheries science, providing key information on growth, age, and population dynamics (Cheung et al., 2007; Ebener et al., 2005; Klumb et al., 1999). In coregonid fish, scale analysis has proven particularly effective for age determination and growth back-calculation (Mills and Beamish, 1980; Muir et al., 2008; Van Oosten, 1923). In current practice, each fish scale must be manually examined under a stereomicroscope, requiring substantial expertise and a significant investment of time and labour. Not every scale of an individual fish is equally readable, necessitating the examination of multiple scales per fish to obtain valid assessments of age

* Corresponding author at: Ludwig-Maximilians-Universität München, Faculty of Biology Department II, Aquatic Ecology, Großhaderner Str. 2, 82152 Planegg-Martinsried, Germany.

E-mail addresses: c.vogelmann@lmu.de, christian.vogelmann@lfl.bayern.de (C. Vogelmann), chris@schock-ing.de (C. Schock), software@feilhauer.de (M. Feilhauer).

https://doi.org/10.1016/j.ecoinf.2025.103517
Received 23 October 2024; Received in revised form 7 November 2025; Accepted 7 November 2025
Available online 11 November 2025

or other necessary measurement parameters (Elzey et al., 2014). Manual scale analysis is therefore widely recognized as a time-consuming and labor-intensive process, often requiring multiple rounds of examination and quality control (Kočovský and Carline, 2000; Ndjamba et al., 2022). The interpretation of scale characteristics is also susceptible to observer bias and inconsistency, particularly for challenging samples or species with complex growth patterns (Long et al., 2018; Peterson et al., 2021; Riedel and Leaf, 2024).

Traditional approaches to age determination and growth back-calculation rely entirely on manual identification of annuli and circuli on each scale. However, differences in how individual readers interpret or measure these ring structures can lead to variation in the estimated age and, consequently, in back-calculated length and weight. Such subjectivity can introduce inconsistencies among studies or monitoring programs, especially when multiple analysts or laboratories are involved.

To address these challenges, recent research has increasingly focused on automating aspects of age and growth estimation from fish scales and otoliths. Automation approaches, including image analysis and machine learning, have shown considerable promise in reducing subjectivity, increasing reproducibility, and enhancing efficiency (Moen et al., 2018; Politikos et al., 2022; Riedel and Leaf, 2024). Notable examples include neural network-based approaches for otolith and scale analysis (Moen et al., 2018; Ordoñez et al., 2020), web-based tools for automated age determination (Politikos et al., 2022), and systems that assist users interactively (Claramunt and Clapp, 2005; Vabø et al., 2021). However, most automated systems developed to date are limited to structure-specific age assignment and typically analyze only a single scale or otolith per image, often without providing comprehensive measurements of other biologically relevant parameters.

There is thus a need for flexible and robust automated solutions that can process multiple scales per scan and extract a wider range of growth parameters – including area, radius, length, width, and circuli count - in a standardized, reproducible manner. The present approach addresses this gap by visualizing scale image analysis results based on definable and robust criteria and thresholds, while allowing for manual verification and correction by the operator. Unlike existing approaches, our newly developed algorithm enables the segmentation and automated analysis of multiple scales per scan, and provides simultaneous measurement of key morphological parameters, including scale area, radius, length, width, and circuli count. This combined approach increases efficiency- reducing processing time from hours to minutes - and standardizes the extraction of biologically relevant features, while reducing observer-related error.

The software-based methodology presented here aims (1) to save working time, thereby enabling the efficient analysis of large numbers of fish scales and growth parameters, and (2) to reduce observer errors occurring during manual inspection of scales under a microscope. By combining automated parameter extraction with operator review, the method increases both the efficiency and reproducibility of fish scale analysis, thereby supporting large-scale ecological and management studies. Ultimately, the method should substantially expand the use of fish scales for estimating fish population dynamics, which is important for the sustainable management of economically significant fish stocks. The benefits of automation for reducing processing time and minimizing labor costs are further addressed in the Discussion, where a direct comparison between manual and automated workflows is provided.

2. Material and procedures

2.1. Study site and sample collection

Lake Starnberg is a large, deep pre-alpine monomitic lake in southern Germany with an area of 56.4 km^2 and a maximum depth of 127 m (Riedmüller et al., 2022). The lake is characterized by cold, oligotrophic waters and supports a natural population of coregonid fish, which are of high ecological and fisheries management importance. Fish were measured to the nearest millimeter for fork length, weighed, and scales were always sampled from the same anatomical location—the anal scale, situated just above the anal fin—to ensure comparability across samples and individuals (Einsele, 1943; Lehtonen and Niemelä, 1998).

2.2. Datasets and analytical approach

Two independent datasets were used to evaluate and demonstrate the performance of the automated scale analysis software:

2.2.1. Method Validation Dataset

A subset of 84 fish (covering a range of lengths, weights, and age classes) from autumn 2020 and 2022 was randomly selected for direct, paired method validation. For each fish, a single scale was measured for total area and circuli count using traditional manual methods (under a stereomicroscope, with area measured by counting graph paper boxes and circuli counted from center to edge). The exact same scales were then scanned and analyzed using a custom-developed algorithm (see below). This experimental design enabled a direct, within-object comparison between manual and automated methods for these key parameters, with manual measurements serving as the reference for validation as defined by Campana (2001).

2.2.2. Ecological Application Dataset

To assess the performance of the automated approach in an applied, representative context, a second, independent dataset was used. This consisted of 124 pelagic fish, all of which had been pre-selected as age 3+ by two independent analysts based on conventional criteria. These fish were sampled annually in autumn between 1998 and 2020 in Lake Starnberg, with 5 to 9 individuals collected per year using standardized pelagic gillnet fishing in open water. For each fish, up to 10 scales were digitized and analyzed. The automated software was first applied to each scale for center detection and annulus identification. Subsequently, both the automatically detected center and all annuli were manually verified and, if necessary, corrected. All subsequent scale parameters (circuli, radius, circuli distance, back-calculated length and weight) were then derived based on these automated or manually verified structures. Metadata for each fish (capture date, length [cm], weight [g]) were encoded in the filename during digitization. This process provided a robust test of the automated system's performance under real-world conditions, while the step of manual review corresponds to the "verification" concept as defined by Campana (2001). Full metadata for all fish and scales are available in the supplemental material.

2.3. Scale preparation and digitization

Collected scales were cleaned using a mild detergent (Pril) and gentle rubbing between thumb and forefinger to remove mucus and debris.

For the ecological application dataset (124 fish sampled between 1998 and 2020), up to 10 scales per fish were mounted flat under a cover glass to avoid measurement errors due to scale curvature, then digitized using a slide scanner (Reflecta CrystalScan 7200) at a resolution of 3600 dpi, producing high-quality grayscale images suitable for automated analysis (Fig. 1A). The number of scales per scan was limited to a maximum of 10, as placing more scales would result in contact or overlap between scales, potentially impairing accurate detection and analysis by the software.

For the validation dataset (84 fish from 2020 and 2022), a single scale per fish was selected and processed in the same way (cleaned, mounted flat, and digitized at 3600 dpi) to enable direct, paired comparisons between manual and automated measurements.

2.4. Statistical analyses and method verification

To assess the performance of the automated approach, paired

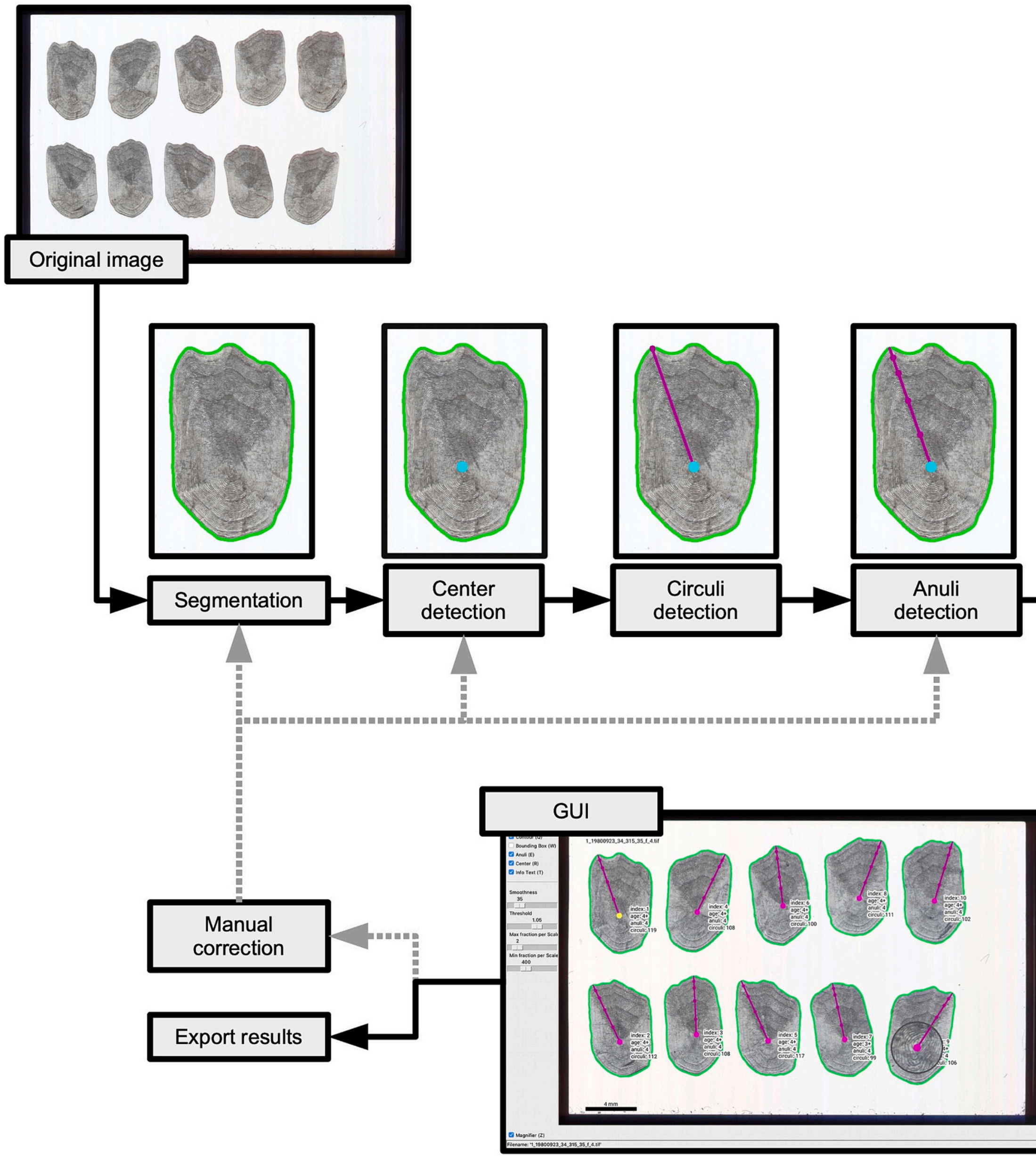

Fig. 1. Workflow of automated scale analysis and options for manual correction using the graphical user interface. Representative digitized images of 10 coregonid fish scales from a single individual caught in Lake Starnberg in 1998 and images showing the results for the single steps of the algorithm (segmentation, center detection, circuli detection and annuli detection) for one exemplary scale.

(within-object) comparisons were conducted for both datasets:

- In the validation dataset, manual measurements were directly compared to automated results for each scale.
- In the verification dataset (field application), all relevant scale parameters were first determined fully automatically. Next, the automatically detected center and annuli were manually reviewed and corrected where needed, and all parameters were then recalculated based on these verified structures. Both sets of results—fully automated and manually verified—were retained and directly compared for each scale, allowing a paired assessment of agreement and differences introduced by manual verification.

All statistical analyses and visualizations were performed in R version 4.2.3. The main packages used were *dplyr*, *ggplot2*, *tidyr*, *viridis*, *patchwork*, and *BlandAltmanLeh*; a complete list of packages is provided in the Supplementary Materials. For each parameter—including number of circuli, circuli distance, radius, annuli, and back-calculated length and weight—descriptive statistics were calculated: mean, standard deviation (SD), mean absolute and relative error, mean difference (bias), and 95 % limits of agreement (LoA; calculated as bias $\pm 1.96 \times$ SD of the paired differences following the Bland–Altman method). Bias was defined as the mean difference between automated and manually verified measurements. The 95 % LoA were used following Bland and Altman (1986) to evaluate the agreement between both methods, providing a direct measure of interchangeability beyond correlation.

All comparisons between automated and manual measurements were performed using untransformed, directly measured values, as the aim was to evaluate agreement between true measurement outputs rather than model-derived residuals. Data transformation was therefore not required. Back-calculated length and weight values were derived from allometric relationships based on measured scale radius and verified annuli counts, which represent biologically derived results rather than statistically transformed variables.

Prior to formal statistical tests, the distribution of paired differences was checked for normality using the Shapiro–Wilk test. Depending on the distribution, statistical significance was assessed using a paired *t*-test (if normally distributed) or a Wilcoxon signed-rank test (if non-normal). Results were considered significant at $p < 0.05$.

For the validation dataset ($n = 84$), linear regression models were fitted for area and circuli count (manual as predictor, automated as response), with regression coefficients, Pearson's.

r, and R^2 reported.

Linear regression and Pearson's r are standard measures in method-comparison studies, providing an interpretable assessment of the strength and linearity of association across the observed range (Bland and Altman, 1986).

To quantify the agreement between automatically detected and manually verified scale centers, we calculated the Euclidean distance between the respective center coordinates (x, y) for each scale. All center coordinates were initially determined in pixels. For consistency in reporting and interpretation, these pixel distances were subsequently converted to millimeters using the scanner resolution (3600 dpi; 1 pixel = 0.00706 mm).

For each scale, we further assessed the difference between the automatically detected and the manually verified centers using paired differences (in pixels), the mean bias, limits of agreement (LoA), and error statistics. The statistical significance of observed differences was evaluated using the Wilcoxon signed-rank test.

2.5. Software

The core of the software is an algorithm applied to the grayscale image. First individual scales within the digital image get recognized and segmented (Fig. 1). Based on the segmentation the circumference and area for each detected scale are calculated. Afterwards the scale center and the maximum radius are determined for each scale individually. This information is then used to identify the circuli and annuli. The algorithm is implemented using the Python programming language in combination with the widely known openCV library for image processing.

The aim was to develop software capable of simultaneous, automatic capture, and analysis of up to 10 coregonid fish scales. The software is designed to facilitate automatic and interactive analysis. We implemented a graphical user interface (gui) that enables the user to load single files or directories. The user can choose between a non - interactive mode and an interactive mode. In non - interactive mode all loaded files will be analyzed and results saved without any user interaction needed, making it ideal for batch processing of large datasets. In interactive mode, the user can review the results in an interactive window and adapt them directly in the image if needed. Overlayed information (i.e. contours, bounding boxes, info text, center and annuli for each scale) can be toggled with simple shortcuts (Fig. 1B, C, D, E). The area around the courser can be magnified to enable the user to work with the highest image resolution available (Fig. 2). The center can be set manually. This automatically updates the circuli count and annuli detection as well as age estimation and back-calculations for the specific scale. In the same way, annuli can be set and erased by simply clicking

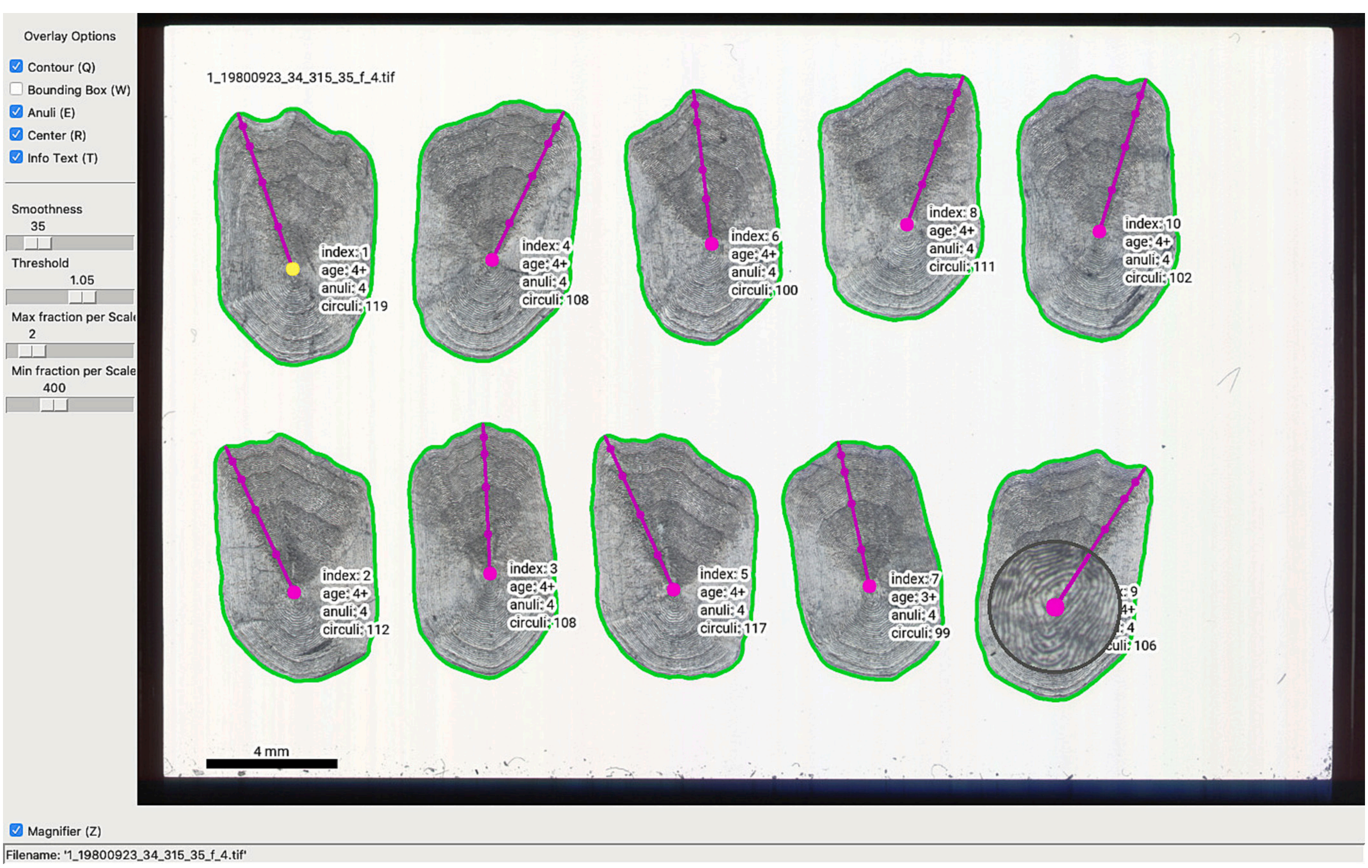

Fig. 2. Automated analysis of coregonid fish scales.
Representative results from the automatic evaluation of 10 coregonid fish scales from the same fish caught in Lake Starnberg 1998 using the Coregon Analyzer software. The scale in the lower right panel is shown as a reference, with the automatically detected center highlighted in yellow (magnified for clarity). Annuli (annual growth rings) are detected along the longest radius from the center to the scale edge and are marked as points. (For interpretation of the references to colour in this figure legend, the reader is referred to the web version of this article.)

on them. After reviewing the results (image with overlay as shown in the interactive window and csv file with all results) can be saved for future inspection and/or analysis (Fig. 2). Not all scales of a fish are consistently readable; therefore, up to 10 scales per fish are digitized and analyzed. To get a robust estimate, we choose a reference scale by comparing the number of validated annuli for each scale and looking for the median from the number of annuli (Fig. 2). If more than one scale has this number of annuli, we look at the circuli for all these scales and take the median of the circuli likewise. The age estimation for the reference scale is used as the age estimation for this fish.

If the center or annuli is set manually for any scale, this scale is automatically set as a reference scale, as the annuli can be considered to be validated by an expert. Still, age estimations for each single scale are outputted in the result files.

2.6. Steps of automatic image analysis

2.6.1. Upload of images

Images in tif or jpeg format are loaded, and information (i.e. date of catch, length and weight at capture) from the filename is parsed for further use in the back-calculations. Input images are converted to grayscale for faster computation where needed.

Date: YYYYMMDD.

Length: [cm].

Weight: [g].

2.6.2. Segmentation of single scales

The input images are filtered with a Gaussian blur and thresholded with an adaptive threshold for segmentation of the single scales (Fig. 1B). Using a blurred image makes the segmentation more robust with respect to noise and rugged edges of the scales. The edges are thereby smoothed out. The intensity of smoothing can be adapted in the GUI. Detected segments that are too large or too small are considered to be noise, dirt, or other structural elements in the images (e.g., dark image frames). The thresholds for those sizes can be adapted in the GUI if needed.

2.6.3. Basic scale analysis

Basic geometric data are calculated directly from the detected scales. Those include the contour, perimeter, area, width, length (Fig. 1B, C, E) and bounding box of each single scale.

2.6.4. Center detection

To find a center, we consider the cropped image of a single scale. This image is rotated so that the boundary box is oriented horizontally. As images are represented as matrices of gray values, we can now calculate the circuli for each column, which is equivalent to drawing vertical lines over the image and calculating circuli for this line. The resulting circuli counts are stored in a 1-D array which is low-pass filtered to find the maximal circuli count. The index of the column with the maximum represents the coordinate of the column in the center. The same is done for each row to calculate the row coordinate of the center. A similar approach for the detection of centers in images of tree cross sections using Sobel and other filters can be found in Gillert et al. (2023). The approach used in this work splits the algorithm into two parts where only the circuli detection has to use the whole image data and the consecutive filtering can be done on the resulting 1-D areas making it fast and especially well suited for processing of large data sets or responsive user interfaces (Fig. 1D; Fig. 2).

With a known center, the point on the contour with the largest distance is calculated and used for further analysis (e.g., for radius, circuli, etc.). This offers a well-defined and user-independent method for calculating the radius.

2.6.5. Circuli detection

Counting circuli can be achieved by analyzing the gray values along a given line in the image. Therefore, lines are defined, and gray values are extracted from the image. We extract values along the line from the given center to the edge of the scale (longest radius) (Fig. 3). Relative minima of those values are considered as circuli. A similar method was employed by Szedlmayer et al. (1991).

2.6.6. Identification of annuli

For each single scale, the circuli from center to edge are differentiated to get the circuli distances between each consecutive circuli (Fig. 1E). From this the local circuli distance is calculated by circuli_density(r) = 1/circuli_distance(r) r being the radius ranging from 0 (=center) to r_max (=edge). The density is forward-backward filtered with a butterworth bandpass filter and then used to find local maxima. Each point having a filtered density value greater than the values of its 30 neighbouring points is considered an annulus candidate. The number of neighbours (i.e. 30) as well as the filter parameters have been manually tuned to fit the given image resolution and the expected distance between annuli.

In a second step, minimal circuli for each year are defined. We choose 15, 20, 20, 10 as minimal numbers of circuli for the corresponding years 1, 2, 3, 4. For all following years, we choose 10 as a minimal number of circuli between consecutive annuli. These values are chosen from experience with this specific species and lake and represent an expected minimal annual growth. If needed these values can be changed by a user to adopt for different locality or species. Starting from the center, we choose the first annulus candidate that has at least the specified number of circuli between itself and the last detected annulus. Iterating over all annulus candidates filters out those candidates that are in too close range of each other (Fig. 4).

2.6.7. Estimation of age

Using the marked annuli, we can get an age estimation for each scale. Each validated annulus represents one year of growth, but annuli near the edge have to be handled differently depending on the date of capture. By calculating the circuli between the outermost annulus and the edge of the scale and checking whether this number is smaller than a given number (8 circuli in this case), we specify whether this annulus is considered to be ‘close’ to the edge (Fig. 5). If an annulus is close to the edge and the fish was captured before May, we assume that growth has not started this year; therefore, the age estimation is the number of annuli. If the fish was captured in May or later, we assume that the annulus at the edge already marks the end of growth for this year there, for the estimated age is age = annuli - 1 but we append a ‘+’ to mark the growth for this year as usual.

If, on the other hand, the last validated annulus is not close to the edge (there are at least 8 circuli between the last annulus and the edge of the scale), we also have to consider the date of capture. If the fish was captured before May, the circuli on the edge are likely to be from last year but the annulus on the edge is not yet clearly formed (or was not detected). Therefore, the estimated age is annuli+1. If the fish was captured in May or later, we assume that the circuli at the edge show the growth of this year and define the age as the number of annuli with an attached ‘+’.

2.6.8. Back-calculations

For each analyzed scale, the software automatically detects all annuli and calculates the corresponding annulus radii as the distances from the determined center to each annulus. The number of circuli per year is calculated by counting all circuli between the center and the first annulus (first year), and between consecutive annuli for subsequent years. The average circuli distance per year is computed as the distance divided by the number of circuli in each annual segment.

Back-calculation of area, length, and weight:

The software enables the reconstruction of historic fish length, weight, and scale area for each year of life, based on the detected annuli. These calculations are performed using both the standard (Lea-Dahl)

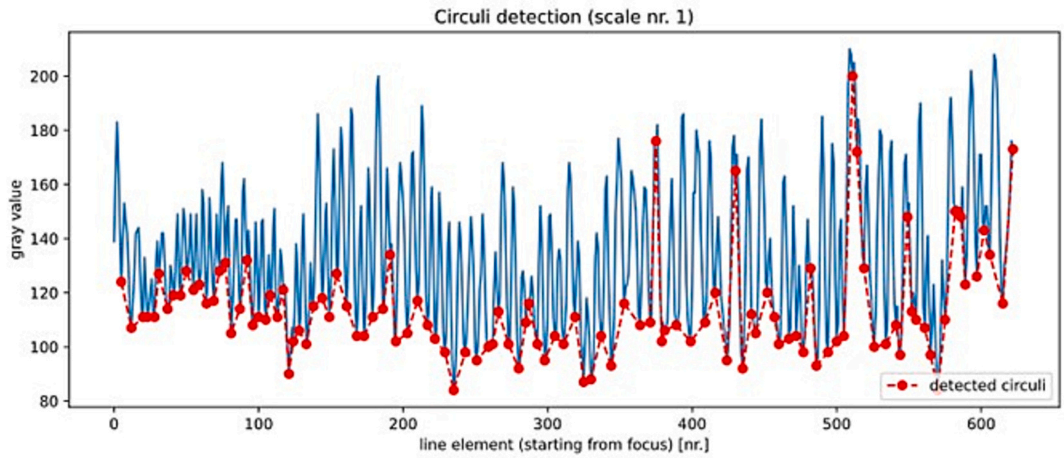

Fig. 3. Automated circuli detection along the longest scale radius. Gray values were extracted along a user-defined line from the detected scale center to the outer margin, representing the longest radius. Relative minima in the gray value profile (blue line) correspond to individual circuli, which are marked by red dots. (For interpretation of the references to colour in this figure legend, the reader is referred to the web version of this article.)

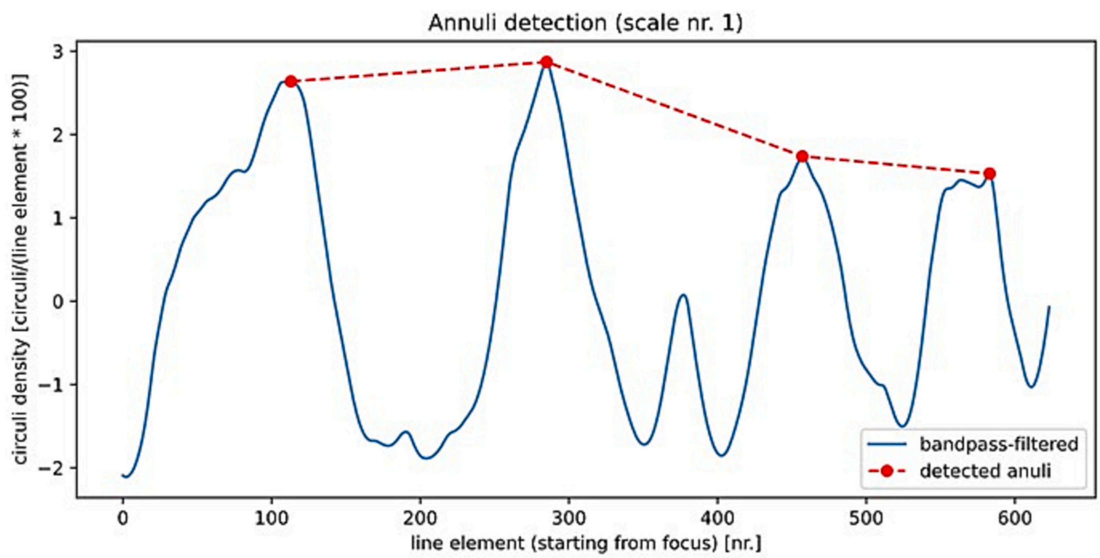

Fig. 4. Automated annulus detection along the longest scale radius.
The blue line shows the bandpass-filtered circuli density profile (calculated as the inverse distance between consecutive circuli) along the longest radius of the scale. Local maxima in the filtered density (red dots) are identified as annulus candidates, corresponding to annual growth rings. Thresholds for minimum circuli count per year are used to refine candidate selection, ensuring biologically plausible annulus detection for the focal species and study site. (For interpretation of the references to colour in this figure legend, the reader is referred to the web version of this article.)

and alternative (Monastyrsky) approaches, with the option for users to select or supply custom parameters (Vigliola and Meekan, 2009).

The area per year is calculated by scaling the area of the scale quadratic with the radius for each year (Eq. 1):

$$\mathrm{area}_{\mathrm{year}} = \left(\mathrm{r}_{\mathrm{year}}/\mathrm{r}_{\mathrm{max}}\right)^2 \text{ x } \mathrm{area}_{\mathrm{max}} \tag{1}$$

with $\mathrm{area}_{\mathrm{max}}$ being the area of the scale at the date of capture, $\mathrm{r}_{\mathrm{max}}$ being the maximum distance from the center to the edge of the scale, and $\mathrm{r}_{(\mathrm{year})}$ being the radius of the detected annulus for the corresponding year.

The length of the fish per year is calculated by scaling the length of the fish with the radius for each year (Eq. 2). Alternatively, the fish length is back-calculated by fitting a curve through the known points for fish length at capture and the corresponding $\mathrm{r}_{\mathrm{max}}$ (Eq. 3) (Vigliola and Meekan, 2009).

$$\text{length}: \mathrm{L}_{\mathrm{year}} = \left(r_{year}/r_{max}\right) \text{ x } L_{capture} \text{ (Lea Dahl)} \tag{2}$$

$$\text{length alternative}: \mathrm{L}_{\mathrm{year\_Mona}} = \left(\mathrm{r}_{\mathrm{year}}/\mathrm{r}_{\mathrm{max}}\right)\mathrm{c} \text{ x } \mathrm{L}_{\mathrm{capture}} \text{ (Monastyrsky)} \tag{3}$$

The weight of the *fish* per year is calculated back by scaling the weight of the fish at capture cubic with the radius per year (Eq. 4). Alternatively, the fish weight is back-calculated by fitting a curve through the known weight at capture (Eq. 5) (Vigliola and Meekan, 2009).

$$\text{weight}: \mathrm{W}_{year} = \left(r_{year}/r_{max}\right)^3 \text{ x } W_{capture} \text{ (Standard)} \tag{4}$$

$$\text{weight alternative}: \mathrm{W}_{years} = \left(r_{year}/r_{max}\right)^{c\_weigth} \text{ x } W_{capture} \text{ (Alternative)} \tag{5}$$

with r_{year}, L_{year}, W_{year} being radius, length, and weight at the corresponding age, $L_{capture}$ and $W_{captureI}$ being the measured length and weight at catch and r_{year} being the automatically detected or manually corrected

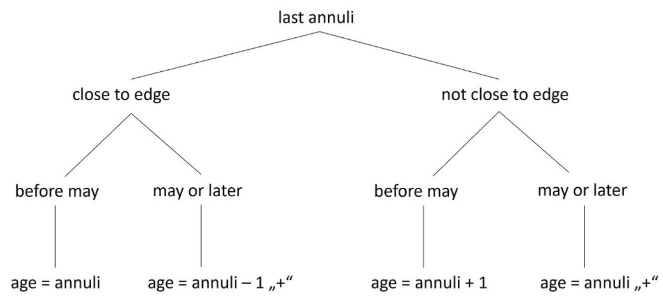

Fig. 5. Decision tree for age assignment based on annuli position and date of capture. Age estimation from fish scales considers both the proximity of the last validated annulus to the scale edge and the date of fish capture. If the outermost annulus is close to the edge (fewer than 8 circuli between annulus and edge), the age is set equal to the number of annuli if the fish was captured before May; if captured in May or later, the age is reduced by one and a '+' is appended to indicate ongoing annual growth. If the last annulus is not close to the edge, age is increased by one for captures before May, or a '+' is appended for captures in May or later, reflecting the possibility of an unformed or undetected annulus. This procedure standardizes age estimates according to the biological and seasonal context.

radius for the corresponding year.

These equations (Eqs. 1–5) are implemented directly in the software to enable transparent, standardized, and reproducible back-calculations of historical fish length, weight, and scale area.

2.6.9. Custom parameterization and default values

All formula parameters (such as exponents c for length or weight) can be customized by the user via a configuration file. If no local data are available, the software provides robust default settings for all formulas. In this study, these default exponents were derived from regressions based on a comprehensive dataset of 1021 coregonid individuals (age classes 1+ to 7+) from Lake Starnberg, Germany. These default values can serve as a starting point, but users are encouraged to generate and use their own regression parameters if local fish populations differ substantially.

To generate custom parameters, users can assemble their own regression dataset: collecting fish of different sizes, measuring length and weight, and digitizing the associated scales. Regression models between scale radius and body size or weight can then be used to update the configuration file, ensuring optimal accuracy for local populations.

2.6.10. Flexibility and transparency

This approach ensures maximum transparency and flexibility: the calculation process is standardized and reproducible, while local adaptation is easily achieved. The method and code thus enable both direct comparability across studies and full customization for new datasets or fish populations.

All datasets, analysis scripts for result reproduction, and the algorithm are publicly available (see Data Availability). The compiled software application can be obtained from the authors upon reasonable request.

3. Results

3.1. Direct comparison of manual and automated area and circuli count

A direct paired comparison was conducted for 84 scales, each measured manually (under a stereomicroscope) and automatically (software-based). Table 1 summarizes regression parameters, agreement statistics, and paired test results.

For scale area [mm^2], the regression slope was 1.03 (95 % confidence interval (CI): 0.98 to 1.08), the intercept 0.81 (95 % CI: −0.33 to 1.94), with $r = 0.97$ ($R^2 = 0.95$). The mean bias was 1.41 mm^2 (95 % LoA: −0.47 to 3.29 mm^2). Both the Wilcoxon signed-rank test and the paired *t*-test indicated significant differences ($p < 0.001$). The differences were not normally distributed (Shapiro–Wilk $p < 0.001$) (Fig. 6, A).

For circuli count, regression analysis yielded a slope of 0.82 (95 % CI: 0.68 to 0.97), intercept 18.20 (95 % CI: 5.74 to 30.65), $r = 0.78$ ($R^2 = 0.60$), mean bias 3.25 (LoA: −11.81 to 18.31). Differences were significant (Wilcoxon and t-test $p < 0.001$) but normally distributed (Shapiro–Wilk $p = 0.61$) (Fig. 6, B).

3.2. Center detection

Automatic detection of the scale center was successful without manual adjustment in 77.9 % (853 out of 1095) of all analyzed scales (Fig. 7A). Only 22.1 % (242 out of 1095) required any manual correction. In nearly all of these cases, the adjustment was minimal: the mean center correction was 0.15 mm (median: 0 mm; maximum: 14.6 mm), and only 7.6 % of scales required a correction greater than 0.5 mm.

The histogram of center deviations (Fig. 7B) shows a pronounced peak at 0 mm, highlighting the high reliability of the automatic center detection. Table 1 summarizes the agreement between automatic and manually verified center positions, with a low mean bias for the X coordinate (0.029 mm, limits of agreement: −0.579 mm to 0.903 mm) and the Y coordinate (0.014 mm, LoA: −1.462 mm to 2.113 mm), as well as low mean absolute errors (0.082 mm and 0.109 mm, respectively). Although the Wilcoxon test indicated statistical significance for both coordinates ($p < 0.05$), the effect size was negligible given the overall scale of measurement.

Outliers with errors greater than 0.5 mm were rare (7.6 %) and typically associated with problematic image quality or atypical scale structures.

3.3. Paired analysis of all scale parameters

Table 2 summarizes paired comparisons for all verified (manual) and automated measurements across 1095 scales. For each parameter, mean, SD, mean absolute and relative error, bias (mean difference), 95 % limits of agreement (LoA), and statistical test results (Wilcoxon signed-rank test) are provided.

3.3.1. Circuli count

For main growth metrics, such as total number of circuli, the mean bias was −1.10 (LoA: −14.63 to 12.43; relative error: 2.1 %). Circuli counts by growth year (circuli r1–r3) showed minor mean biases (see

Table 1
Comparison of manual and automated scale area and circuli counts.*, *, *

Parameter	n	Slope (95 % CI)	Intercept (95 % CI)	r	R^2	Bias	LoA lower	LoA upper	Wilc. p	t-test p
Scale area [mm^2]	84	1.03 (0.98, 1.08)	0.81 (−0.33, 1.94)	0.97	0.95	1.41	−0.47	3.29	<0.001	<0.001
Circuli count [n]	84	0.82 (0.68, 0.97)	18.20 (5.74, 30.65)	0.78	0.60	3.25	−11.81	18.31	<0.001	<0.001

Regression coefficients (with 95 % confidence intervals), Pearson correlation (r), coefficient of determination (R^2), bias, and 95 % limits of agreement (LoA) are shown. All p-values refer to two-sided paired tests (Wilcoxon (Wilc.) signed-rank and paired t-test). Wilc. = Wilcoxon signed-rank test; CI = confidence interval.

* Bias and limits of agreement (LoA) were calculated according to the Bland–Altman method.

* r = Pearson's correlation coefficient; R^2 = coefficient of determination.

* CI = confidence interval; LoA = limits of agreement; Wilc. = Wilcoxon signed-rank test.

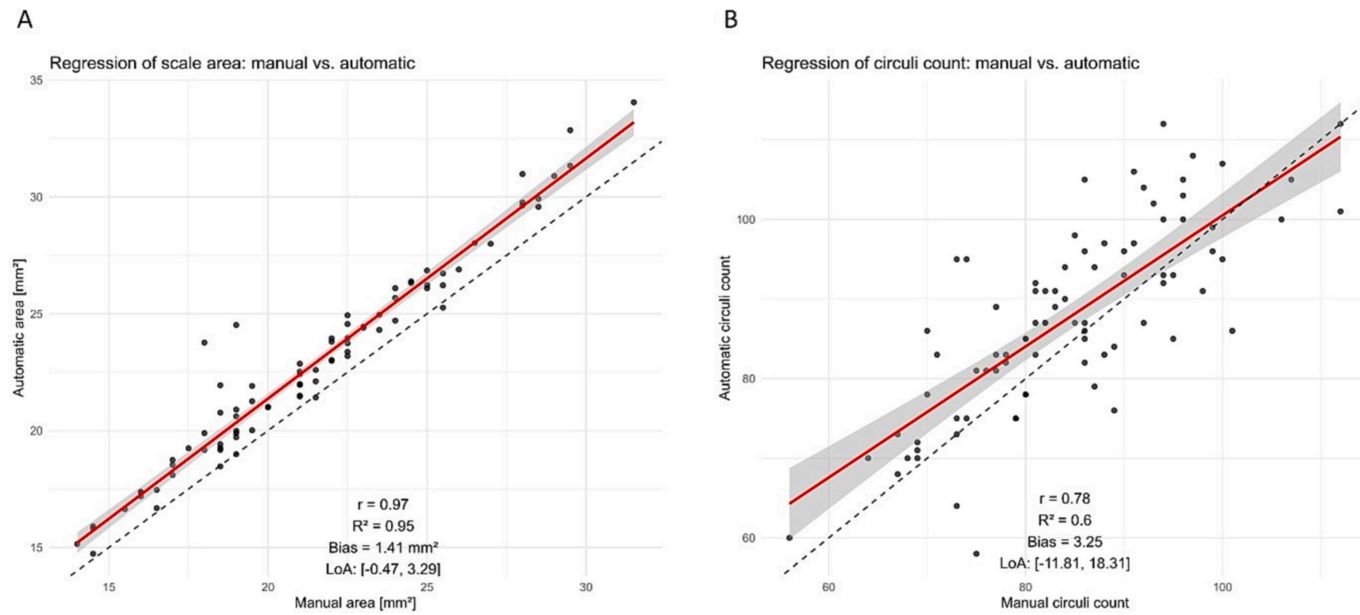

Fig. 6. Comparison of manual and automatic measurements for individually analyzed coregonid scales (n = 84) from Lake Starnberg (2020−2022). (A) Regression of scale area measurements [mm^2]. (B) Regression of circuli counts. The solid red line shows the fitted regression with 95 % confidence interval (gray), the dashed line indicates the 1:1 relationship. Statistical parameters (correlation coefficient, R^2, mean bias, and limits of agreement) are provided for each panel. r = Pearson's correlation coefficient; LoA = 95 % limits of agreement (Bland–Altman method). (For interpretation of the references to colour in this figure legend, the reader is referred to the web version of this article.)

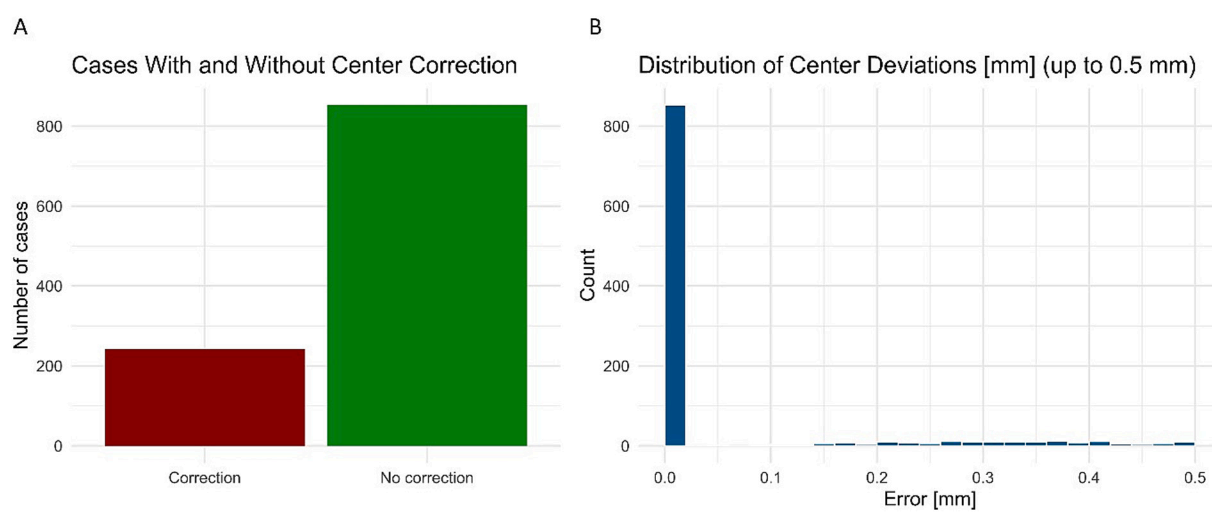

Fig. 7. (A) Number of fish scales for which the automatically detected center was accepted without manual correction ("No correction") or required manual adjustment ("Correction") during verification (n = 1095). (B) Distribution of Euclidean distances between automatic and manually verified centers (in mm). Histogram displays only deviations ≤0.5 mm; most corrections were minimal.

Table 1), with statistically significant differences for r2 and r3 (p < 0.001). However, the absolute differences were small relative to the observed SD (Table 2; Fig. 8A).

3.3.2. Radius measurement

For scale radii (r1, r2, r3, r_max), mean biases were below 0.1 mm (except r_max: −0.04 mm; LoA: −0.54 to 0.47 mm; relative error: 1.6 %). For most parameters, Wilcoxon test p-values were significant (Table 2), but effect sizes were minor (Table 3; Fig. 8B).

3.3.3. Circuli distance

Paired analysis of circuli spacing (distances r1–r3) showed mean biases below 0.001 mm, with relative errors of 4–5 %. For r1 and r3, differences were statistically significant, but not for r2 (Table 2; Fig. 8C).

3.3.4. Annuli detection

For annulus count, the mean bias was 0.24 (LoA: −1.45 to 1.94; relative error: 19.5 %), with a significant difference detected by the Wilcoxon test (p < 0.001). Median counts did not differ between methods (Table 2; Fig. 8D).

3.3.5. Length and weight back-calculations

For the back-calculation of fish length and weight, both standard and alternative formulas were applied (see Methods for details). In both approaches, the automated software calculated all values using either the automatically determined or, when necessary, the manually verified center position on the scale. This allows a direct comparison of the impact of center correction on subsequent length and weight estimates (Table 3).

Table 2
Paired comparison of manual and automatic measurements for key scale parameters. For each parameter, sample size (N), mean, standard deviation (SD), minimum and maximum values, mean absolute error, mean relative error (%), bias (mean difference), limits of agreement (LoA), statistical test used, and p-value are reported.*

Parameter	N	Mean man.	SD man.	Min man.	Max man.	Mean auto	SD auto	Min auto	Max auto	Abs. Error	Rel. Error (%)	Bias	LoA lower	LoA upper	p-value
annuli	1095	3.2	0.5	1.0	6.0	3.4	0.9	2.0	10.0	0.6	19.5	0.2	−1.5	1.9	<0.001*, *, *, * and *
center_x	1095	2583.7	1250.6	460.0	4764.0	2587.8	1251.0	511.0	4764.0	11.6	0.6	4.1	−82.0	90.3	0.001**
center_y	1095	1650.1	722.9	477.0	2868.0	1652.1	721.2	477.0	2868.0	15.4	1.3	2.0	−207.2	211.3	<0.001**
circuli	1095	100.0	11.6	64.0	152.0	98.9	12.4	64.0	213.0	2.2	2.1	−1.1	−14.6	12.4	<0.001**
circuli_dist_r1	1095	0.04	0.00	0.03	0.06	0.04	0.00	0.03	0.05	0.00	4.1	0.00	−0.01	0.01	<0.001**
circuli_dist_r2	1094	0.04	0.00	0.03	0.06	0.04	0.00	0.03	0.07	0.00	5.5	0.00	−0.01	0.01	0.20
circuli_dist_r3	922	0.05	0.01	0.03	0.07	0.05	0.01	0.03	0.07	0.00	4.4	0.00	−0.01	0.01	0.01*
circuli_r1	1095	27.2	7.5	12.0	87.0	27.5	9.6	15.0	69.0	5.9	22.5	0.3	−19.3	20.0	0.45
circuli_r2	1094	31.9	8.7	11.0	64.0	29.8	6.9	19.0	55.0	6.5	20.7	−2.2	−21.7	17.3	<0.001**
circuli_r3	922	26.2	7.3	7.0	50.0	28.5	6.5	19.0	54.0	5.8	27.6	2.3	−14.6	19.3	<0.001**
r1	1095	1.0	0.3	0.4	3.6	1.0	0.4	0.5	2.6	0.2	24.5	0.0	−0.8	0.8	0.10
r2	1094	2.4	0.5	0.9	4.7	2.3	0.5	1.2	4.4	0.4	17.8	−0.1	−1.3	1.2	<0.01**
r3	922	3.6	0.5	1.7	5.6	3.5	0.5	2.1	5.4	0.3	9.3	−0.1	−1.1	1.0	<0.001**
r_max	1095	4.3	0.5	2.7	6.3	4.2	0.5	2.7	9.4	0.1	1.6	−0.0	−0.5	0.5	<0.001**

* All tests were performed as paired Wilcoxon signed-rank tests (due to non-normal distribution of differences).
* All values are based on paired measurements of n = [number] fish scales unless otherwise indicated.
* Boldface indicates statistically significant p-values ($p < 0.05$). Abbreviations: man. = manual; auto = automatic; Abs. Error = mean absolute error; Rel. Error = mean relative error; Bias = mean difference (auto – manual); LoA = limits of agreement (Bias ± 1.96 × SD of the differences).
* Units: r1, r2, r3, r_max = mm; circuli_, annuli, circuli = count; circuli_dist_ = mm; center_x, center_y = pixels.
* dist = mean circuli distance per annual segment (mm); r1, r2, r3 = radii from the scale center to the 1st, 2nd, and 3rd annulus, respectively (mm); r_max = maximum radius from the scale center to the outer edge of the scale (mm).

Across all calculated length parameters (r1–r3, alternative r1–r3), mean biases between manual verification and the fully automatic workflow were generally low, typically below 0.5 mm for most years. Relative errors ranged from 9 % to 29 %, with slightly higher variation observed in the first back-calculation year. For weight parameters (r1–r3, alternative r1–r3), the mean absolute error varied more strongly but generally remained within the expected biological range for the species and age group. Relative errors for weight were naturally higher, particularly in the earliest growth years due to low absolute values.

Most paired Wilcoxon signed-rank tests indicated no statistically significant differences between the methods, with *p*-values exceeding the 0.05 threshold for the majority of parameters. Where significant differences were observed (see Table 2), the effect sizes were small and are unlikely to affect ecological interpretations or management decisions. Notably, for length and weight at capture, both methods yielded identical values, resulting in zero bias and error, as expected from the data structure.

Taken together, these results demonstrate that both the standard and alternative back-calculation approaches implemented in the software yield highly consistent outcomes, regardless of whether the scale center was determined automatically or after manual correction. Thus, the software provides reliable back-calculated length and weight values suitable for use in fisheries monitoring and ecological research. A complete overview of all paired results, including significant *p*-values (bold), is provided in Table 3.

4. Discussion

Digitalization approaches aiding in fish scale analysis have been investigated in numerous studies (Fablet, 2006; Frie, 1982; Szedlmayer et al., 1991). Automated determination approaches, such as those of Politikos et al. (2022), yield promising results for age determination. Also noteworthy is the approach of Moen et al. (2018), which employs deep learning for the determination of the age of the fish. In addition, recent studies highlight the potential of automated and semi-automated systems to reduce observer bias and increase processing throughput (Ordoñez et al., 2020; Riedel and Leaf, 2024). The clear advantage of this automated workflow is that it not only automatically generates parameters such as circuli count, spacing, radius measurements, annulus detection, age determination, and length and weight recalculations, but also allows for interactive intervention of the user allowing correction if necessary. This combination of comprehensive parameterization and optional user verification is not available in previous systems and directly addresses the needs for transparency and flexibility in long-term ecological studies.

4.1. Comparison between manual vs. automated measurements

Based on the validation dataset ($n = 84$), direct paired comparison of manually and automatically determined scale area revealed a very high degree of agreement (Fig. 6A). The correlation coefficient between methods was $r = 0.97$, and the mean difference (bias) was 1.41 mm^2, with automated measurements tending to produce slightly higher area values. This small positive bias is likely attributable to the flattening of scales between glass slides during scanning, which ensures a standardized two-dimensional measurement. In contrast, manual area measurment under the stereomicroscope can be affected by incomplete flattening, potentially leading to marginal underestimation due to the three-dimensional curvature of the scales.

For the total circuli count (Fig. 6B), agreement between methods was substantial ($r = 0.78$, bias = 3.25). Some variation was observed, which may result from subjective differences in identifying and counting circuli under the microscope, as well as from the automated algorithm's handling of ambiguous or partially obscured rings. Both approaches are challenged by variability in scale quality, such as the presence of dried epidermal tissue or irregular growth patterns, which can affect both manual and automated detection.

Despite these challenges, the observed differences between manual and automated measurements were generally small relative to the range of observed values and are unlikely to affect biological interpretations in the context of population monitoring (Ordoñez et al., 2020; Politikos et al., 2022).

4.2. Center detection

According to the current state of knowledge, there is no existing software capable of automatically detecting the center of coregonid fish scales. In this study, the automated algorithm demonstrated a high

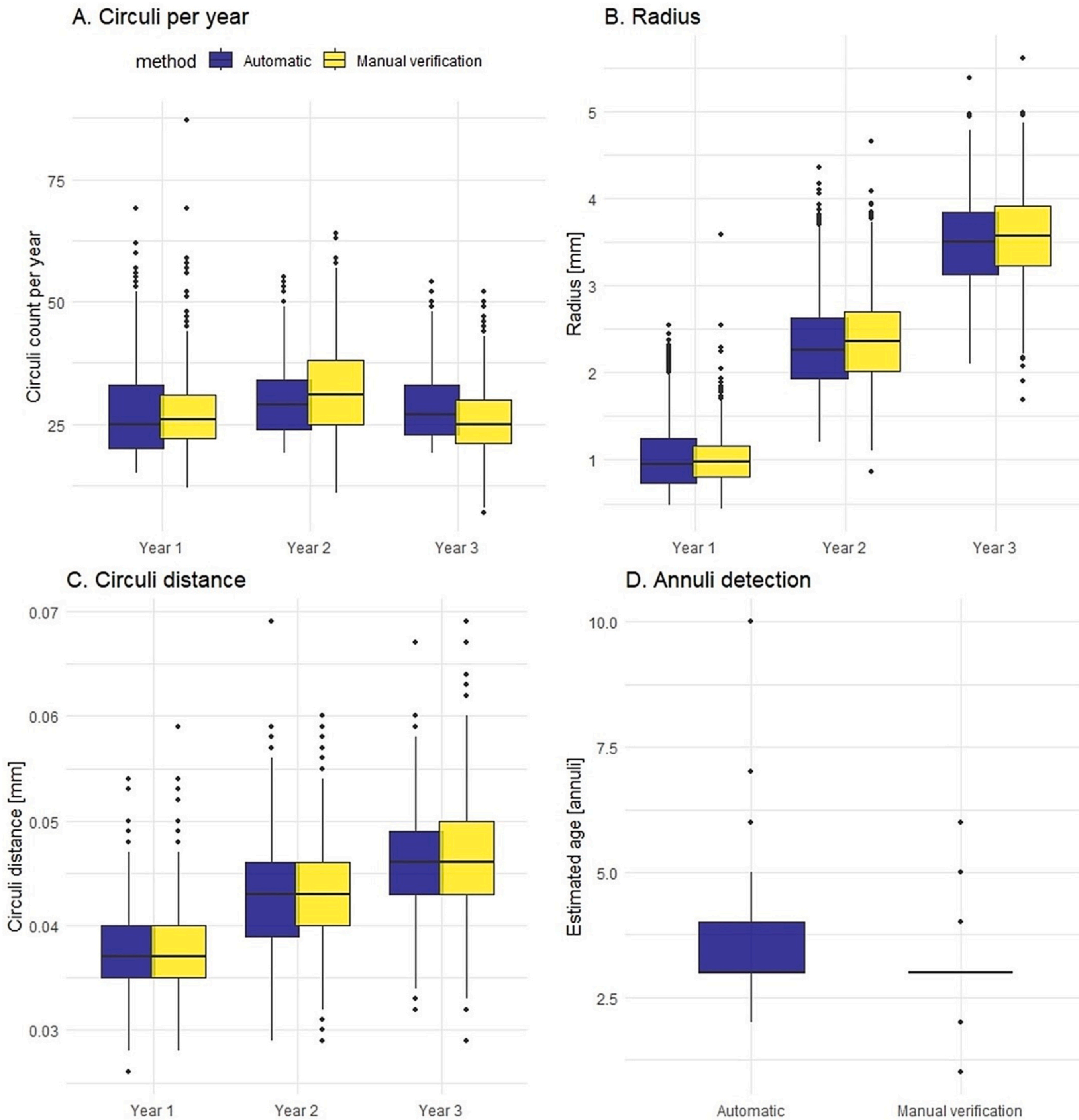

Fig. 8. Paired comparison of key scale parameters estimated by manual verification (blue) and automated analysis (yellow) for coregonid fish (n = 1095 scales). Panels show: (A) Circuli count per year, (B) Radius [mm], (C) Circuli distance [mm], and (D) Annuli detection (estimated age). Manual verification represents interactive user correction of automated results; automatic denotes fully automated extraction. In each box, the horizontal line represents the median, the lower and upper hinges correspond to the first and third quartiles, whiskers extend to 1.5 × the interquartile range, and small circles indicate outliers. (For interpretation of the references to colour in this figure legend, the reader is referred to the web version of this article.)

degree of reliability: for 77.9 % of the 1095 analyzed scales, the automatically detected center was accepted without any manual adjustment (Fig. 7A). In the remaining 22.1 % of cases, manual correction was necessary, but the required adjustment was typically minimal. The distribution of center deviations (Fig. 7B) is sharply peaked at zero, with a mean correction of only 0.15 mm (median: 0 mm). Only 7.6 % of all scales required a correction exceeding 0.5 mm.

The few outlier corrections observed were almost exclusively associated with technical issues, such as adjacent scales coming into contact during scanning. In such cases, the algorithm occasionally assigned the center to the wrong structure, resulting in a large deviation. These rare instances aside, the agreement between automatic and manually verified centers was consistently close, as shown by the low mean bias and absolute error in Table 1.

Accurate center detection is critical, as all subsequent morphometric analyses—such as measurements of scale radius, circuli count and

Table 3
Comparison of back-calculated length and weight using validated (manually verified center) and fully automatic scale analyses. For each parameter, sample size (N), mean, standard deviation (SD), minimum and maximum values, mean absolute error, mean relative error (%), bias (mean difference), limits of agreement (LoA), statistical test used, and p-value are reported.

Parameter	N	Mean man.	SD man.	Min man.	Max man.	Mean auto	SD auto	Min auto	Max auto	Abs. Error	Rel. Error (%)	Bias	LoA lower	LoA upper	p-value
length_alt_r1	1095	6.2	2.1	0.0	25.7	6.6	3.1	0.0	19.5	1.7	29.2	0.4	−5.6	6.4	<0.01*, *, *, *, * and *
length_alt_r2	1094	16.4	4.0	0.0	31.1	16.3	5.0	0.0	33.2	3.3	20.7	−0.1	−10.4	10.1	0.19
length_alt_r3	922	25.6	4.3	0.0	34.3	25.2	4.8	0.0	34.3	2.5	10.4	−0.4	−8.6	7.9	<0.01**
length_r1	1095	7.4	2.2	0.0	26.3	7.8	3.2	0.0	20.7	1.8	25.3	0.4	−5.8	6.6	<0.01**
length_r2	1094	17.6	3.8	0.0	31.2	17.4	4.8	0.0	33.4	3.1	18.2	−0.1	−9.9	9.6	0.17
length_r3	922	26.1	4.1	0.0	34.5	25.8	4.5	0.0	34.5	2.3	9.2	−0.4	−7.9	7.2	<0.01**
weight_alt_r1	1095	13.4	10.5	0.0	171.4	16.3	15.7	0.0	109.5	7.9	76.0	2.9	−29.0	34.8	<0.01**
weight_alt_r2	1094	80.9	36.9	0.0	302.8	82.2	50.3	0.0	358.9	31.5	44.2	1.4	−102.7	105.4	0.44
weight_alt_r3	922	187.0	62.3	0.0	412.2	182.4	66.8	0.0	391.0	34.0	20.0	−4.6	−116.8	107.7	0.02*
weight_r1	1095	4.5	6.5	0.0	144.1	6.3	9.0	−0.2	69.6	4.1	155.7	1.9	−17.5	21.3	<0.001**
weight_r2	1094	52.1	32.4	0.0	276.7	55.2	48.0	−4.5	338.5	28.9	72.8	3.1	−97.0	103.2	0.56
weight_r3	922	162.3	62.1	0.0	371.1	158.1	70.3	−11.1	383.2	39.6	29.1	−4.2	−133.2	124.9	0.03*

* Back-calculations were performed automatically in both cases, but for the validated dataset, center placement and annulus detection were manually verified before automated analysis. In the automated dataset, all steps were fully automated without user intervention.
* All tests were performed as paired Wilcoxon signed-rank tests (due to non-normal distribution of differences).
* All values are based on paired measurements of n = [number] fish scales unless otherwise indicated.
* Boldface indicates statistically significant p-values ($p < 0.05$). Abbreviations: man. = manual; auto = automated; Abs. Error = mean absolute error; Rel. Error = mean relative error; Bias = mean difference (auto – manual); LoA = limits of agreement (Bias ± 1.96 × SD of the differences).
* Units: length_ = mm; weight_ = g.
* r1, r2, r3 = radii from the scale center to the 1st, 2nd, and 3rd annulus, respectively (mm); r_max = maximum scale radius (mm); alt = alternative back-calculation method (Monastyrsky).

spacing, and annulus detection—depend on correct center placement. The minimal corrections required in most cases demonstrate that the automated approach provides a robust and efficient solution for high-throughput scale analysis, with manual intervention only rarely needed and mostly limited to problematic images. This greatly accelerates the analysis process while maintaining high data quality.

Manual center placement is traditionally considered time-consuming and subject to individual interpretation, which can introduce observer bias and variability (Kočovský and Carline, 2000; Long et al., 2018; Ndjamba et al., 2022). The automated approach provides a standardized and reproducible method, ensuring consistency across large datasets and among different users. As a result, robust and objective scale measurements can be obtained with minimal manual intervention, significantly improving both efficiency and data quality in fish scale analysis.

4.3. Circuli-count,-distance, and radius detection

Cycloid scales of whitefish form circuli during growth, which spread concentrically from the center (Schönbörner et al., 1979). These patterns—circuli count, spacing, and radius—can provide detailed information on growth, physiological stress, and environmental effects (Cheung et al., 2007; Peterson et al., 2014). The automated extraction of circuli count produced results that closely matched manual verification counts (mean bias: −1.10; relative error: 2.1 %; Table 2). This agreement is within the expected range of variability found among different experienced readers (Long et al., 2018; Phelps et al., 2007; Piferrer and Anastasiadi, 2023). As previously described, some discrepancies occurred in samples where two scales were scanned together or where intermediate rings were present (Fig. 8). This is a known challenge in manual analysis as well and has been reported to contribute to variability in age and growth studies (Campana, 2001; Ndjamba et al., 2022). Distance between circuli, a proxy for growth increments, showed excellent agreement between manual verification and automated approaches (relative error typically <6 %; Table 2). Cheung et al. (2007) and Garcia-Fernández et al. (2022) have suggested that circuli spacing can be a sensitive indicator of rapid or reduced growth. Our results demonstrate that automated analysis enables the standardized and reproducible measurement of circuli spacing across large datasets, which is a key prerequisite for robust comparative growth analyses. By reducing subjective estimation, the software enables high-throughput and repeatable measurement of these fine-scale growth features. The maximum radius of a scale is an established indicator of fish size and past growth (Reckahn, 1986; Peterson et al., 2014; Walker and Sutton, 2016). The present results show a minimal bias (−0.04 mm; relative error 1.6 %), confirming that the automated method reliably detects the radius even across large sample sizes (Table 1). Minor deviations primarily reflect differences in scale flatness between manual and automated preparations, as noted in Kočovský and Carline (2000). Fig. 8B provides a direct comparison of radius estimates by method for each year.

Initial approaches to automated scale analysis (e.g., Szedlmayer et al., 1991) often lacked the ability to measure all relevant parameters in parallel or required extensive manual intervention. The present software advances this field by enabling the simultaneous and objective measurement of circuli count, distance, and radius for each digitized scale in a single step. This comprehensive, reproducible dataset supports advanced analysis of fish growth, stress, and population dynamics—significantly enhancing the utility of scale analysis for fisheries science and management (Beakes et al., 2014; Bigelow and White, 1996; Bilton and Robins, 1971; Talbot and Doyle, 1992). Full paired results for circuli count, spacing, and scale radius are provided in Table 2, enabling transparent measurement of agreement and error structure across the entire dataset. A visual summary of these results, including all outliers and method-specific distributions, is presented in Fig. 8 (panels A-C).

Importantly, circuli count and spacing are gaining attention as proxies for historical growth and environmental change (e.g., Thomas et al., 2019). Experimental studies have shown that both metrics can sensitively indicate variability in temperature and food availability, with circuli number and spacing reflecting both growth rates and environmental stressors. However, as Thomas et al. (2019) highlight, spacing may not always directly mirror somatic growth, particularly under fluctuating conditions. Narrowly spaced circuli can occur during periods of both rapid and reduced growth, depending on temperature and feeding regime.

In this context, our automated approach enables reproducible and unbiased quantification of these key scale metrics across large datasets, supporting both fisheries management and ecological studies addressing climate-driven changes in fish growth.

4.4. Annuli detection

Scales are a widely used structure for age determination in coregonid fish and provide essential information for population assessment and management (Muir et al., 2008; Van Oosten, 1923). The determination of age from scales under a stereomicroscope is a standard method, but it is time-consuming and subject to variability arising from analyst expertise, preparation technique, and environmental factors that can influence scale structure. For example, intermediate or double rings can develop, potentially leading to age overestimation (Campana, 2005). These challenges, including subjectivity and inter-reader variability, have been highlighted in several comparative studies of age determination (Elzey et al., 2014; Oele et al., 2015).

In this study, we compared automated annulus detection to manual verification (see Methods). The results demonstrate that the automated software generally yields annulus counts close to those obtained manually (Fig. 8D). Table 2 presents all key metrics for annulus detection. No systematic bias was found, and all deviations can be explained by known methodological differences. Our findings align with previous work showing that automated approaches can produce age estimates comparable to those derived from human analysts, while improving efficiency and consistency (Ordoñez et al., 2020; Politikos et al., 2022). The observed differences can be attributed to methodological differences: during manual verification, all visible rings, including partially formed (intermediate or double) rings, were often counted or marked by the analyst. In contrast, the automated approach applies predefined thresholds for the minimum number of circuli between annuli, causing some ambiguous rings to be overlooked by the algorithm. As a result, automated detection criteria may sometimes lead to systematic differences in age assignments compared to manual readings, especially in the presence of ambiguous or poorly defined structures (Moen et al., 2018; Ordoñez et al., 2020).

On average, automated detection tends to result in slightly higher age estimates (by approximately 0.2 years for 3+ fish in this dataset; see Table 2). While the mean number of annuli is slightly higher for the automated method (3.4 vs. 3.2). Although the difference is statistically significant ($p < 0.001$), the overall biological interpretation remains comparable for most individuals, as both methods identify the same age class in the majority of cases. Visual differences can be seen in some cases, primarily due to ambiguous or intermediate rings.

Overall, these findings confirm that automated analysis provides robust annulus detection for large-scale monitoring while reducing subjectivity and analyst dependency (Ordoñez et al., 2020; Politikos et al., 2022). Where discrepancies occur, they can typically be explained by methodological differences in ring interpretation rather than substantive biological divergence (Oele et al., 2015).

Outliers visible in Fig. 8D, where a small number of scales show exceptionally high or low annulus counts, were primarily associated with problematic samples. For example, in one extreme case, the automated algorithm detected up to 10 annuli on a single scale; manual inspection revealed that two scales were inadvertently overlapping, causing the algorithm to interpret them as a single object with excessive rings. Other outliers arose in scales with poor quality due to contamination, remnants of epidermal tissue, or ambiguous ring structures. Such conditions posed challenges for both automated and manual measurement.

Additionally, the boxplot distribution reflects that manual verification sometimes resulted in slightly higher or lower annulus counts compared to the automated method (Fig. 8D). This is mainly because manual readers may choose to mark partial or intermediate rings, which the automated algorithm, using predefined thresholds, is designed to overlook. Consequently, differences in annulus count between the two approaches are largely attributable to these methodological nuances, rather than consistent over- or underestimation by either method.

4.5. Back-calculation

The back-calculation of fish lengths and weights is of great importance in fisheries management, as it provides key information on individual and population growth history, health status, and biomass estimates (Klumb et al., 1999; Muir et al., 2008). Automated analysis facilitates the rapid and consistent reconstruction of historical length and weight at age for large sample sets, making high-throughput monitoring feasible (Politikos et al., 2022).

In this study, length and weight at age were back-calculated for all individuals using both automated and manually verified annulus detection. For example, the mean absolute error in back-calculated length across all annuli ranged from 1.7 to 3.3 mm, with relative errors typically below 30 %. Differences in weight estimates were slightly higher for younger ageclasses but converged for older age classes (Table 3). While some differences between manual and automated methods were statistically significant (e.g., length at r1, $p < 0.01$), the overall magnitude of these differences remained small relative to the biological variability observed in the dataset. This allows readers to assess method performance across different models and supports population-specific customization as described in the methods section. Our approach produced back-calculated values that were generally consistent with those obtained from manual verification, with small differences depending primarily on which back-calculation formula was applied. The choice of model and the precision of annulus detection can significantly influence length and weight estimates, especially in early life stages (Britton, 2007; Busst and Britton, 2014; Piferrer and Anastasiadi, 2023).

As highlighted by recent work (Han et al., 2025), model selection and the precision of annulus detection are especially critical for back-calculation in younger fish, where growth increments are small and error margins correspondingly large. Our results reflect this pattern, with both absolute and relative errors being highest for age-1 and age-2 fish (Table 3). This methodological uncertainty is well documented in the literature and is not unique to scales, but also affects other structures such as otoliths (Campana, 2001; Han et al., 2025). These limitations are particularly relevant in the context of fisheries-induced evolution (FIE), where systematic biases or reduced precision in early growth estimates can compound over time and affect both management decisions and the interpretation of long-term population trends.

4.6. Efficiency, standardization, and advantages of automation

Manual age and growth analysis of fish scales is a well-established but extremely time-consuming and error-prone process, heavily dependent on reader expertise and consistency (Britton, 2007; Isermann et al., 2003; Kočovský and Carline, 2000; Long et al., 2018; Ndjamba et al., 2022; Riedel and Leaf, 2024). In our study, manual measurement of just 84 scales required approximately 16 working hours, whereas the automated workflow—including scanning, analysis, and verification—reduced the processing time for the entire field dataset of 124 fish (1095 scales) to less than nine hours. For even larger datasets, this time savings is expected to be even more substantial. Generating all relevant parameters manually—such as radius, perimeter, length, width, area, total and annual circuli count, and circuli distance—would require many weeks of focused work, especially when preparing data for further statistical analysis.

By contrast, the automated approach presented here enables the rapid, standardized, and reproducible extraction of all relevant parameters, delivering fully formatted results immediately in a CSV file. This not only accelerates processing dramatically but also improves data quality, consistency, and comparability—especially important in long-term or multi-operator studies.

A key advantage of the workflow is its high degree of flexibility and customization. Users can define and apply water body- or population-specific length–weight relationships directly within the software, supporting accurate, context-specific back-calculation of growth for different populations or environments. This feature is especially valuable when comparing populations from contrasting environments, such as oligotrophic versus eutrophic lakes, where growth trajectories may differ substantially. Model parameters can be adjusted by the user, ensuring the workflow is robust and adaptable for a range of ecological and fisheries management questions.

Unlike many existing automated approaches, which are often limited to single-parameter estimation or do not allow for user verification and correction, our system uniquely combines comprehensive parameter extraction with semi-automated verification. This bridges the gap between accuracy, transparency, and practical application—supporting both efficiency and scientific rigor in long-term monitoring programs (see Tables 1–3).

It should be noted that our present analysis focused on cases with high expert agreement, which allowed for clear benchmarking of the algorithm's performance. Including more ambiguous or challenging samples, where experts may disagree, will be an important direction for future research and further refinement of the system.

In summary, the automated system presented here enables high-throughput processing, reliable standardization, and essential customization, supporting comprehensive, reproducible, and context-appropriate scale analysis for both ecological and fisheries management purposes.

4.7. Limitations and applicability

The present version of the automated scale analysis software was developed and validated for *coregonid* scales, which exhibit cycloid structures with clearly defined annuli and circuli suitable for automated detection. Consequently, the current implementation is species-specific and optimized for this morphology. However, since the underlying image-processing workflow—comprising segmentation, center and radius detection, and annulus and circulus recognition—relies on generalizable geometric and textural features, the framework is conceptually transferable to other species that possess similar scale types. Future adaptations may involve parameter adjustment or retraining to account for species-specific differences in scale size, curvature, or pattern expression.

Additionally, as with any image-based approach, results depend on the quality of scanned material, illumination, and preparation consistency. These factors, along with sample size and scale preservation, may influence detection accuracy and should be considered when applying the method to new datasets. Despite these limitations, the presented workflow provides a robust foundation for extending automated scale analysis beyond coregonids in future research.

The reliability of scale-based back-calculations also depends on the quality and representativeness of the data used to parameterize length–weight and length–radius relationships. As shown in recent ecological modeling studies (Bouchet et al., 2019; Wang and Jackson, 2023; Yates et al., 2018), sample size, data quality, and model structure can substantially affect predictive performance and transferability. This further underlines the importance of the software's flexible parameterization, which allows users to adapt relationships to local populations and data conditions.

Moreover, the performance of scale-based age and growth estimation may also be influenced by the composition of the underlying data, including disproportionate representation of certain cohorts, uneven age structures, or differing individual growth rates. Populations with skewed age distributions or variable vital rates can exhibit differences in scale clarity and annulus formation, which may affect both annulus detection and back-calculated growth trajectories. These factors highlight the importance of considering cohort structure and population dynamics when applying scale-based analyses, and they underscore the value of future work aimed at evaluating the method across populations with different demographic and ecological characteristics (Tucker et al., 2024; Wang et al., 2018).

5. Conclusions

Continuous monitoring is a fundamental requirement for assessing the status of fish populations. To ensure sustainable fisheries management, regular age determination and assessment of growth performance in whitefish are essential. However, the workload associated with these tasks is substantial, often making it difficult to deliver timely results for management and research purposes.

The automated scale analysis software presented here offers a substantial advance, enabling rapid, reproducible, and high-throughput extraction of key scale parameters from digital scans. The workflow allows both fully automated processing and interactive verification, so that results can be reviewed and (where needed) corrected by the user. Direct paired comparison with traditional manual measurements demonstrated that the automated approach delivers highly reliable and accurate results for area, circuli count and annuli. In addition, the automated extraction of radius measurements and the option for direct back-calculation of fish length and weight are important features not provided by most existing programs. This comprehensive parameter set expands the analytical possibilities and offers new opportunities for standardized and reproducible scale analysis in fisheries science.

A key achievement of this study is the successful verification of the software using an ecologically relevant dataset spanning 22 years from Lake Starnberg. This shows that the automated approach is not only technically robust, but also applicable in practical field monitoring of natural fish populations. The digital workflow greatly simplifies data management: digital scans are durable, can be securely archived, and are easily shared for future re-analysis or for collaboration with other research groups.

The software is freely available from the authors upon request. By providing this tool, we aim to support a broader adoption of automated scale analysis in fisheries science and management. In summary, the approach presented here substantially improves efficiency, standardization and data management, enabling more comprehensive and reproducible insights into population dynamics and growth history, both now and for future research questions.

CRediT authorship contribution statement

Christian Vogelmann: Writing – review & editing, Writing – original draft, Visualization, Validation, Supervision, Project administration, Methodology, Investigation, Formal analysis, Data curation, Conceptualization. **Christian Schock:** Writing – review & editing, Visualization, Software, Methodology, Formal analysis. **Marius Feilhauer:** Writing – review & editing, Visualization, Software, Methodology, Formal analysis. **Herwig Stibor:** Writing – review & editing, Writing – original draft, Conceptualization. **Michael Schubert:** Writing – review & editing, Project administration, Methodology, Conceptualization.

Funding

This study was financially supported by the Bavarian State Ministry of Food, Agriculture, and Forestry (StMELF).

Declaration of competing interest

Christian Vogelmann reports financial support was provided by Bavarian State Ministry of Food, Agriculture, and Forestry (StMELF). If there are other authors, they declare that they have no known competing financial interests or personal relationships that could have appeared to influence the work reported in this paper.

Data availability

The data supporting the findings of this study are openly available on Figshare at: https://doi.org/10.6084/m9.figshare.29467970

Additionally, the R code used for data analysis and figure generation is available on GitHub at: https://github.com/Birdy332/Automatic-fish-scale-analysis-r-scripts

The complete Coregon Analyzer software (incl. GUI and pre-processing tools) is available from the authors upon request under a research-use license.

References

Beakes, M.P., Sharron, S., Charish, R., Moore, J.W., Satterthwaite, W.H., Sturm, E., et al., 2014. Using scale characteristics and water temperature to reconstruct growth rates of juvenile steelhead Oncorhynchus mykiss: SCALE DEVELOPMENT OF ONCORHYNCHUS MYKISS. J. Fish Biol. 84 (1), 58–72. https://doi.org/10.1111/jfb.12254.

Bigelow, P.E., White, R.G., 1996. Evaluation of growth interruption as a means of manipulat-ing scale patterns for mass-marking hatchery trout. N. Am. J. Fish Manag. 16 (1), 142–153. https://doi.org/10.1577/1548-8675(1996)016<0142:EOGIAA>2.3.CO;2.

Bilton, H.T., Robins, G.L., 1971. Effects of starvation, feeding, and light period on circulus for-mation on scales of young sockeye salmon (Oncorhynchus nerka). Can. J. Fish. Aquat. Sci. 28 (11), 1749–1755. https://doi.org/10.1139/f71-259.

Bland, J.M., Altman, D.G., 1986. Statistical methods for assessing agreement between two methods of clinical measurement. Lancet 327 (8476), 307–310. https://doi.org/10.1016/S0140-6736(86)90837-8.

Bouchet, P.J., Peterson, A.T., Zurell, D., et al., 2019. Better model transfers require knowledge of mechanisms. Trends Ecol. Evol. 34, 489–490. https://doi.org/10.1016/j.tree.2019.04.006.

Britton, J.R., 2007. Reference data for evaluating the growth of common riverine fishes in the UK. J. Appl. Ichthyol. 23, 555–560. https://doi.org/10.1111/j.1439-0426.2007.00845.x.

Busst, G.M.A., Britton, J.R., 2014. Precision of the age–length increments of three cyprinids: effects of fish number and sub-sampling strategy. J. Fish Biol. 84 (6), 1926–1939. https://doi.org/10.1111/jfb.12409.

Campana, S.E., 2001. Accuracy, precision, and quality control in age determination, including a review of the use and abuse of age validation methods. J. Fish Biol. 59, 197–242.

Campana, S.E., 2005. Otolith science entering the 21st century. Mar. Freshw. Res. 56 (5), 485. https://doi.org/10.1071/MF04147.

Cheung, C.H.Y., Chaillé, P.M., Randall, D.J., Gray, J.S., Au, D.W.T., 2007. The use of scale increment as a means of indicating fish growth and growth impairment. Aquaculture 266 (1–4), 102–111. https://doi.org/10.1016/j.aquaculture.2007.02.036.

Claramunt, R.M., Clapp, D.F., 2005. Image Analysis Procedures for Aging Calcified Structures: An Example with Lake Michigan Lake. Michigan Department of Natural Resources, Fisheries Division, whitefish.

Ebener, M.P., Bence, J.R., Newman, K.R., Schneeberger, P.J., 2005. Application of statisti-cal catch-at-age models to assess lake whitefish stocks in the 1836 treaty-ceded waters of the upper Great Lakes. Proc. Workshop Dynam. Lake Whitefish 271–309.

Einsele, W., 1943. Über das Wachstum der Coregonen im Voralpengebiet, insbesondere über das Verhältnis von Schuppen-und Längenwachstum. Zeitschrift für Fischerei 41 (1), 23–45.

Elzey, S., Rogers, K.A., Trull, K.J., 2014. Comparison of 4 aging structures in the american shad (alosa sapidissima). Fish. Bull. 113 (1), 47–54. https://doi.org/10.7755/fb.113.1.5.

Fablet, R., 2006. Statistical learning applied to computer-assisted fish age and growth estima-tion from otolith images. Fish. Res. 81 (2–3), 219–228. https://doi.org/10.1016/j.fishres.2006.07.013.

Frie, R.V., 1982. Measurement of fish scales and back-calculation of body lengths using a dig-itizing pad and microcomputer. Fisheries 7 (5), 5–8.

Gillert, A., Resente, G., Anadon-Rosell, A., Wilmking, M., Freiherr von Lukas, U., 2023. Iterative Next Boundary Detection for Instance Segmentation of Tree Rings in Microscopy Images of Shrub Cross Sections. https://arxiv.org/abs/2212.03022.

Han, K.Y., Brennan, R.S., Monk, C.T., Jentoft, S., Helmerson, C., Dierking, J., Hüssy, K., Kokubun, É.E., Fuss, J., Krause-Kyora, B., Thomsen, T.B., Heredia, B.D., Reusch, T.B.H., 2025. Genomic evidence for fisheries-induced evolution in Eastern Baltic cod. Sci. Adv. 11, eadr9889. https://doi.org/10.1126/sciadv.adr9889.

Isermann, D.A., Meerbeek, J.R., Scholten, G.D., Willis, D.W., 2003. Evaluation of three different structures used for walleye age estimation with emphasis on removal and processing times. N. Am. J. Fish Manag. 23 (2), 625–631. https://doi.org/10.1577/1548-8675(2003)0232.0.co;2.

Klumb, R.A., Bozek, M.A., Frie, R.V., 1999. Validation of the Dahl–Lea and Fraser–Lee back-calculation models by using oxytetracycline-marked bluegills and bluegill× green sun-fish hybrids. N. Am. J. Fish Manag. 19 (2), 504–514. https://doi.org/10.1577/1548-8675(1999)019<0504:VOTDLA>2.0.CO;2.

Kočovský, P.M., Carline, R.F., 2000. A comparison of methods for estimating ages of unexploited walleyes. N. Am. J. Fish Manag. 20, 1044–1048. https://doi.org/10.1577/1548-8675(2000)020.

Lehtonen, H., Niemelä, E., 1998. Growth and population structure of whitefish (Coregonus lavaretus (L.)) in mountain lakes of northern Finland. Arch. Hydrobiol. 49, 81–95.

Long, J., Holley, C., Taylor, A., 2018. Evaluation of ageing accuracy with complementary non-lethal methods for slow-growing, northern populations of shoal bass. Fish. Manag. Ecol. 25 (2), 150–157. https://doi.org/10.1111/fme.12274.

Mills, K.H., Beamish, R.J., 1980. Comparison of fin-ray and Scale age determinations for Lake whitefish (Coregonus clupeaformis) and their implications for estimates of growth and annual survival. Can. J. Fish. Aquat. Sci. 37 (3), 534–544. https://doi.org/10.1139/f80-068.

Moen, E., Handegard, N.O., Allken, V., Albert, O.T., Harbitz, A., Malde, K., Patterson, H.M., 2018. Automatic interpretation of otoliths using deep learning. PLoS One 13 (12). https://doi.org/10.1371/journal.pone.0204713.

Muir, A.M., Sutton, T.M., Peeters, P.J., Claramunt, R.M., Kinnunen, R.E., 2008. An Evalua-tion of age estimation structures for Lake whitefish in Lake Michigan: selecting an aging method based on precision and a decision analysis. N. Am. J. Fish Manag. 28 (6), 1928–1940. https://doi.org/10.1577/M08-014.1.

Ndjamba, T., Araya, M., Oliva, M., 2022. Otolith weight as an estimator of the age of Seriola lalandi Valenciennes, 1833 (Carangidae), in the southeastern Pacific. Animals 12, 1640. https://doi.org/10.3390/ani12131640.

Oele, D.L., Lawson, Z.J., McIntyre, P.B., 2015. Precision and bias in aging northern pike: comparisons among four calcified structures. N. Am. J. Fish Manag. 35 (6), 1177–1184. https://doi.org/10.1080/02755947.2015.1099579.

Ordoñez, A., Eikvil, L., Salberg, A., Harbitz, A., Murray, S., Kampffmeyer, M., 2020. Explaining decisions of deep neural networks used for fish age prediction. PLoS One 15 (6), e0235013. https://doi.org/10.1371/journal.pone.0235013.

Peterson, E.E., Sheehan, T.F., Zydlewski, J.D., 2021. Scale growth rates and scale circulus deposition rates of marine-stage Atlantic salmon Salmo salar raised under semi-natural con-ditions. J. Northwest Atl. Fish. Sci. 52, 19–27. https://doi.org/10.2960/J.v52.m733.

Phelps, Q.E., Edwards, K.R., Willis, D.W., 2007. Precision of five structures for estimating age of common carp. N. Am. J. Fish Manag. 27, 103–105. https://doi.org/10.1577/M06-045.1.

Piferrer, F., Anastasiadi, D., 2023. Age estimation in fishes using epigenetic clocks: applications to fisheries management and conservation biology. Front. Mar. Sci. 10, 1062151. https://doi.org/10.3389/fmars.2023.1062151.

Politikos, D.V., Sykiniotis, N., Petasis, G., Dedousis, P., Ordoñez, A., Vabø, R., et al., 2022. DeepOtolith v1.0: an open-source AI platform for automating fish age Reading from otolith or scale images. Fishes 7 (3), 121. https://doi.org/10.3390/fishes7030121.

Reckahn, J.A., 1986. Long-term cyclical trends in growth of Lake whitefish in South Bay, Lake Huron. Trans. Am. Fish. Soc. 115 (6), 787–804. https://doi.org/10.1577/1548-8659(1986)115<787:LCTIGO>2.0.CO;2.

Riedel, R., Leaf, R., 2024. Assessing the utility of computer vision for age determination of gulf menhaden. N. Am. J. Fish Manag. 44 (5), 1081–1091. https://doi.org/10.1002/nafm.11039.

Riedmüller, U., Mischke, U., Pottgiesser, T., Böhmer, J., Deneke, R., Ritterbusch, D., Stelzer, D., Hoehn, E., 2022. Steckbriefe der deutschen Seetypen. Begleittext und Steckbriefe.

Schönbörner, A.A., Boivin, G., Baud, C.A., 1979. The mineralization processes in teleost fish scales. Cell Tissue Res. 202 (2). https://doi.org/10.1007/BF00232235.

Szedlmayer, S.T., Szedlmayer, M.M., Sieracki, M.E., 1991. Automated enumeration by com-puter digitization of age-0 weakfish Cynoscion regalis scale circuli. Fish. Bull. 89, 337.

Talbot, A.J., Doyle, R.W., 1992. Statistical interrelation of length, growth, and scale circulus spacing: use of ossification to detect nongrowing fish. Can. J. Fish. Aquat. Sci. 49 (4), 701–707.

Thomas, K., Hansen, T., Brophy, D., Maoiléidigh, Ó., Fjelldal, P.G., 2019. Experimental in-vestigation of the effects of temperature and feeding regime on scale growth in Atlantic salmon *Salmo salar* post-smolts. J. Fish Biol. 94 (6), 896–908. Special Issue: FSBI Sym-posium 2018: The Sustainable Use and Exploitation of Fishes, University of East Anglia, 9–13 July 2018. https://doi.org/10.1111/jfb.13971.

Tucker, C.M., Giacomini, H.C., Mandrak, N.E., et al., 2024. Estimating fish production in wetlands. Can. J. Fish. Aquat. Sci. 81, 847–861. https://doi.org/10.1139/cjfas-2023-0220.

Vabø, R., Moen, E., Smoliński, S., Husebø, Å., Handegard, N.O., Malde, K., 2021. Automatic interpretation of salmon scales using deep learning. Eco. Inform. 63. https://doi.org/10.1016/j.ecoinf.2021.101322.

Van Oosten, J., 1923. A study of the scales of whitefishes of known ages. Zoologica 2 (17), 380–412. Available online. http://pubs.er.usgs.gov/publication/1000458. Accessed on 29. Apr. 2024.

Vigliola, L., Meekan, M.G., 2009. The Back-calculation of fish growth from otoliths. Tropical fish otoliths: information for assessment. Manage. Ecol. 11, 174–211. Available online. http://link.springer.com/10.1007/978-1-4020-5775-5_6. Accessed on 29. Apr. 2024.

Walker, B.M., Sutton, T.M., 2016. Growth-increment formation using otoliths and scales for age-0 Chinook salmon. N. Am. J. Fish Manag. 36 (5), 995–999. https://doi.org/10.1080/02755947.2016.1184202.

Wang, L., Jackson, D.A., 2023. Effects of sample size, data quality, and species response in environmental space on modeling species distributions. Landsc. Ecol. 38, 4009–4031. https://doi.org/10.1007/s10980-023-01771-2.

Wang, X., Wang, L., Lv, S., Li, T., 2018. Stock discrimination and connectivity assessment of yellowfin seabream (Acanthopagrus latus) in northern South China Sea using otolith elemental fingerprints. Saudi J. Biol. Sci. 25, 1163–1169. https://doi.org/10.1016/j.sjbs.2017.09.006.

Yates, K.L., Bouchet, P.J., Caley, M.J., et al., 2018. Outstanding challenges in the transferability of ecological models. Trends Ecol. Evol. 33, 790–802. https://doi.org/10.1016/j.tree.2018.08.001.